Magnetic quantum graphs with time-reversal non-invariant vertex coupling

Marzieh Baradaran

Univerzita Hradec Králové, Czechia

joint work with Pavel Exner and Jiří Lipovský

M. Baradaran, P. Exner, and J. Lipovsky, J. Phys. A: Math. Theor. 55 (2022) 375203.
M. Baradaran, P. Exner, and J. Lipovsky, Ann. Phys. 454 (2023) 169339.
M. Baradaran, and P. Exner, J. Phys. A: Math. Theor. 57 (2024) 265202.

AAMP XXI, Prague, August 29, 2024

Univerzita Hradec Králové
Přírodovědecká fakulta

Quantum graphs

A metric graph consists of a set of edges and vertices; each edge is assigned a positive length ℓ_j and therefore identified with an interval $[0, \ell_j]$.

We associate with the graph the Hilbert space $\mathcal{H} = \bigoplus_{j=1}^{N} L^2([0, \ell_j])$, the elements of which are $\Psi = \{\psi_j\}$.

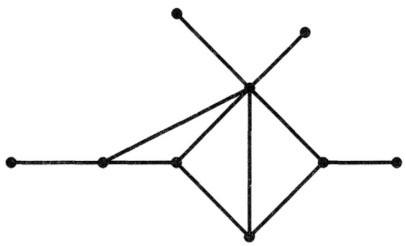

Source: the cited book

G. Berkolaiko, P. Kuchment: *Introduction to Quantum Graphs*, AMS, Providence, R.I., 2013.

Quantum graphs

A metric graph consists of a set of edges and vertices; each edge is assigned a positive length ℓ_j and therefore identified with an interval $[0, \ell_j]$.

We associate with the graph the Hilbert space $\mathcal{H} = \bigoplus_{j=1}^{N} L^2([0, \ell_j])$, the elements of which are $\Psi = \{\psi_j\}$.

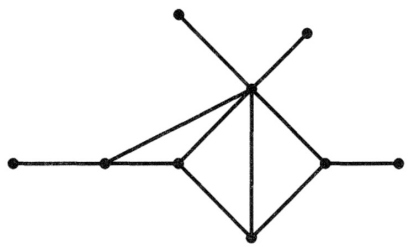

Source: the cited book

Quantum graph is a metric graph equipped with a differential operator (acting on the graph edges) accompanied by appropriate vertex conditions.

- In the presence of a magnetic field, the Hamiltonian acts as the magnetic Laplacian, $(-i\nabla - \mathbf{A})^2$, assuming $\hbar = 2m = 1$.
- To make such a Hamiltonian a self-adjoint operator, one has to match the functions ψ_j properly at each graph vertex.

G. Berkolaiko, P. Kuchment: *Introduction to Quantum Graphs*, AMS, Providence, R.I., 2013.

Vertex coupling

At each vertex v connecting n edges of the graph, the self-adjointness is ensured provided the functions at the vertex are matched through the condition

$$(U - I)\Psi_v + i(U + I)(\mathcal{D}\Psi)_v = 0\,,$$

where U is an $n \times n$ unitary matrix, $\mathcal{D} := \frac{d}{dx} - i\,A_j$ is the quasi-derivative operator, A_j is the tangential component of the magnetic vector potential on the jth edge, Ψ_v and $(\mathcal{D}\Psi)_v$ are the vectors of the boundary values of functions and their (outward) quasi-derivatives.

Vertex coupling

At each vertex v connecting n edges of the graph, the self-adjointness is ensured provided the functions at the vertex are matched through the condition

$$(U - I)\Psi_v + i(U + I)(\mathcal{D}\Psi)_v = 0\,,$$

where U is an $n \times n$ unitary matrix, $\mathcal{D} := \frac{d}{dx} - i\,A_j$ is the quasi-derivative operator, A_j is the tangential component of the magnetic vector potential on the jth edge, Ψ_v and $(\mathcal{D}\Psi)_v$ are the vectors of the boundary values of functions and their (outward) quasi-derivatives.

The most commonly used coupling conditions:

- δ-coupling, and in particular, Dirichlet and Kirchhoff conditions; corresponding to the choice of $U = \frac{2}{n+i\alpha}\mathcal{J} - I$.
- δ'-coupling, and in particular, Neumann and anti-Kirchhoff conditions; corresponding to the choice of $U = I - \frac{2}{n-i\beta}\mathcal{J}$.

Vertex coupling of a preferred-orientation

- introduced by Exner and Tater

P. Exner and M. Tater, Quantum graphs with vertices of a preferred orientation, Phys. Lett. A 382 (2018).

- motivated by the application to model the anomalous Hall effect
- the coupling matrix

$$U = +R := \begin{pmatrix} 0 & 1 & 0 & \dots & 0 & 0 \\ 0 & 0 & 1 & \dots & 0 & 0 \\ \vdots & \vdots & \vdots & \ddots & \vdots & \vdots \\ 0 & 0 & 0 & \dots & 0 & 1 \\ 1 & 0 & 0 & \dots & 0 & 0 \end{pmatrix}$$

Vertex coupling of a preferred-orientation

- introduced by Exner and Tater

P. Exner and M. Tater, Quantum graphs with vertices of a preferred orientation, Phys. Lett. A 382 (2018).

- motivated by the application to model the anomalous Hall effect
- the coupling matrix

$$U = +R := \begin{pmatrix} 0 & 1 & 0 & \dots & 0 & 0 \\ 0 & 0 & 1 & \dots & 0 & 0 \\ \vdots & \vdots & \vdots & \ddots & \vdots & \vdots \\ 0 & 0 & 0 & \dots & 0 & 1 \\ 1 & 0 & 0 & \dots & 0 & 0 \end{pmatrix}$$

In the component form, the conditions (R coupling) are

$$(\psi_{j+1} - \psi_j) + i\,(\mathcal{D}\psi_{j+1} + \mathcal{D}\psi_j) = 0, \qquad j = 1, \dots, n\,,$$

for a vertex of degree n where $\mathcal{D} := \frac{d}{dx} - i\,A_j$.

Asymptotics of the preferred-orientation coupling

The transport properties of the vertex at high energies depend on the vertex parity; the vertex remains transparent if it is of an even parity, while for the odd ones, we get an effective decoupling of the edges.

Asymptotics of the preferred-orientation coupling

The transport properties of the vertex at high energies depend on the vertex parity; the vertex remains transparent if it is of an even parity, while for the odd ones, we get an effective decoupling of the edges.

- Denoting $\eta := \frac{1-k}{1+k}$, a straightforward computation gives [1]

$$S_{ij}(k) = \frac{1-\eta^2}{1-\eta^N}\left\{ -\eta\,\frac{1-\eta^{N-2}}{1-\eta^2}\,\delta_{ij} + (1-\delta_{ij})\,\eta^{(j-i-1)(\mathrm{mod}\ N)} \right\},$$

  in particular,for $N = 3, 4$, we get

$$S_3(k) = \frac{1+\eta}{1+\eta+\eta^2}\begin{pmatrix} \frac{-\eta}{1+\eta} & 1 & \eta \\ \eta & \frac{-\eta}{1+\eta} & 1 \\ 1 & \eta & \frac{-\eta}{1+\eta} \end{pmatrix}, \quad S_4(k) = \frac{1}{1+\eta^2}\begin{pmatrix} -\eta & 1 & \eta & \eta^2 \\ \eta^2 & -\eta & 1 & \eta \\ \eta & \eta^2 & -\eta & 1 \\ 1 & \eta & \eta^2 & -\eta \end{pmatrix}$$

- We see that $\lim_{k\to\infty} S(k) = I$ if N is odd, while for N even the limit is different from the unit matrix.

[1] P. Exner and M. Tater, Phys. Lett. A 382 (2018).

Previous results on preferred-orientation coupling: non-magnetic quantum graphs

- Exner, P., and Tater, M., *Phys. Lett. A* 382 (2018) 283–287.
- Exner, P., and Lipovský, J., *J. Math. Phys.* 60 (2019), 122101.
- Exner, P., and Lipovský, J., *Phys. Lett. A* 384 (2020), 126390.
- Baradaran, M, Exner, P, and Tater, M, *Rev. Math. Phys.* 33 (2021), 2060005.
- Exner, P, *Phys. Part. Nucl.* 52 (2021), 330–336.
- Exner, P., and Tater, M., *Phys. Lett. A* 416 (2021) 127669.
- Baradaran, M, and Exner, P, *J. Math. Phys.* 63 (2022), 083502.
- Baradaran, M., Exner, P., and Tater, M., *Ann. Phys.* 443 (2022), 168992.
- Baradaran, M., and Exner, P., *J. Phys. A: Math. Theor.* 57 (2024), 265202.

- spectral properties of different types of lattices and array of loops
- asymptotic behavior of the spectral bands and transport properties in the high-energy regime

Magnetic generalizations of the previously studied non-magnetic models

P. Baradaran, M., Exner, P., and Tater, M., *Ann. Phys.* 443 (2022), 168992.

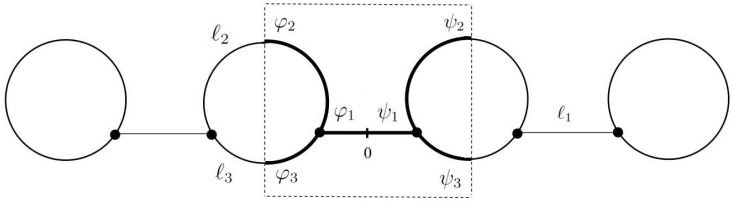

- loosely connected rings ($d_v = 3$): the spectrum is dominated by gaps.

P. Exner and M. Tater, Phys. Lett. A 382 (2018).

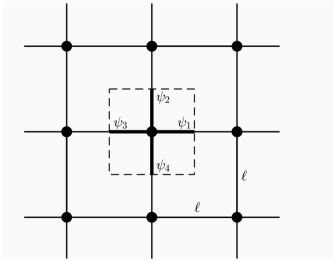

Source: the cited paper

- square lattice ($d_v = 4$): the spectrum is dominated by bands.

Magnetic ring chains

We consider an array of rings, coupled either tightly or loosely through connecting links, in a homogeneous magnetic field $\mathbf{B} = (0, 0, B)$. The magnetic potential is supported on the loops at which the Hamiltonian acts as $\psi_j \mapsto -\mathcal{D}^2\psi_j$ where $\mathcal{D} := \frac{d}{dx} - i\,A_j$.

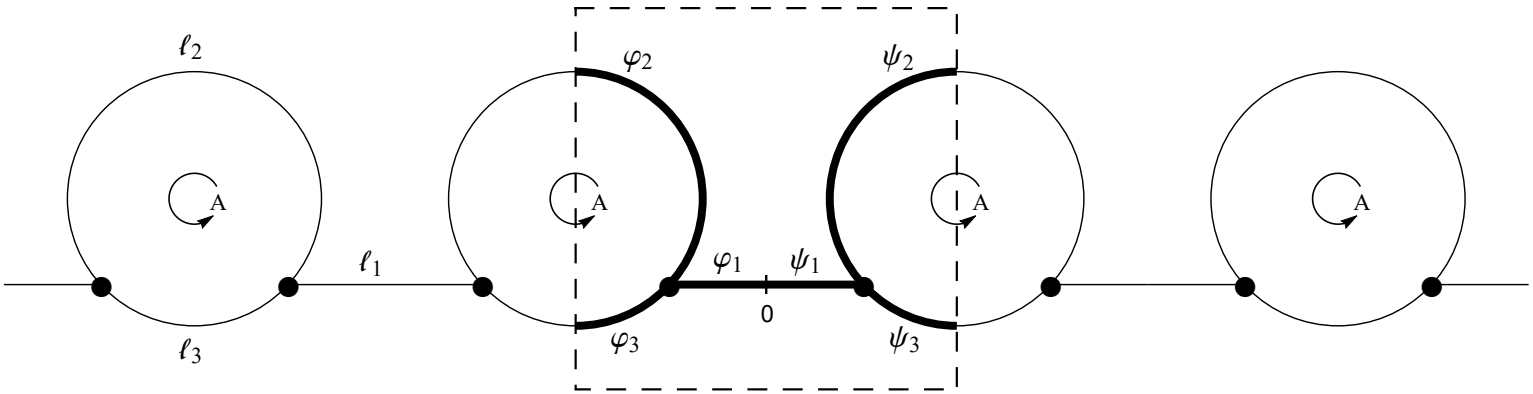

- loosely connected rings, $\ell_i \neq 0$ ($d_v = 3$)
- two limiting cases, $\ell_1 = 0$ or $\ell_2 = 0$ ($d_v = 4$)

Baradaran, M., Exner, P. and Lipovsky, J., J. Phys. A: Math. Theor. 55 (2022) 375203.

Magnetic ring chains

We consider an array of rings, coupled either tightly or loosely through connecting links, in a homogeneous magnetic field $\mathbf{B} = (0, 0, B)$. The magnetic potential is supported on the loops at which the Hamiltonian acts as $\psi_j \mapsto -\mathcal{D}^2\psi_j$ where $\mathcal{D} := \frac{d}{dx} - i\,A_j$.

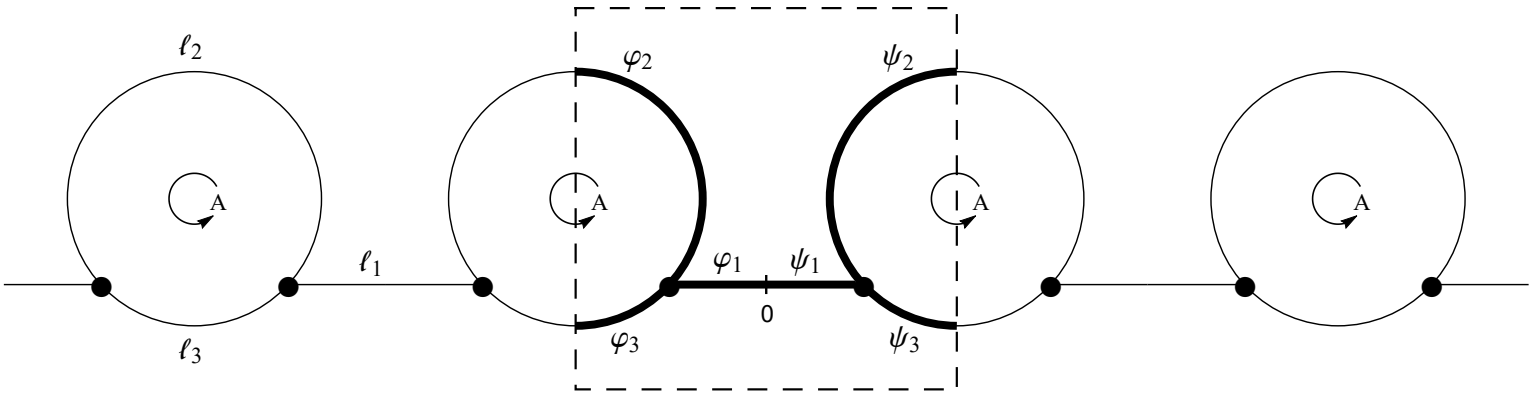

- loosely connected rings, $\ell_i \neq 0$ $(d_v = 3)$
- two limiting cases, $\ell_1 = 0$ or $\ell_2 = 0$ $(d_v = 4)$
- according to Floquet-Bloch decomposition theorem, we consider an elementary cell
- for positive energies $E = k^2 > 0$, the Ansatz for the solution is $\left(a_j^+\, e^{ikx} + a_j^-\, e^{-ikx}\right) e^{i\,A_j\,x}$; for negative energies, one replaces k by $i\kappa$ with $\kappa > 0$

Baradaran, M., Exner, P. and Lipovsky, J., J. Phys. A: Math. Theor. 55 (2022) 375203.

To find the spectral condition, the functions have to be matched through

- the preferred-orientation coupling at each vertex
- Floquet conditions at the free ends of the cell

Theorem (Baradaran, Exner, Lipovsky, 2022)

- For $A \in \mathbb{Z}$, the spectrum is the same as that for non-magnetic chain.
- For $A - \frac{1}{2} \in \mathbb{Z}$, depending on ℓ_i, $i = 1, 3$, flat bands occur at the energies $k^2 = q^2 \left(n - \frac{1}{2}\right)^2$ with $q, n \in \mathbb{N}$ where q is odd.
- Away from those flat bands, the spectrum is absolutely continuous having a band-and-gap structure; it has infinitely many gaps in its positive part.
- The negative spectrum consists of a pair of bands which may merge at particular values of the parameters.

- we have the following spectral patterns

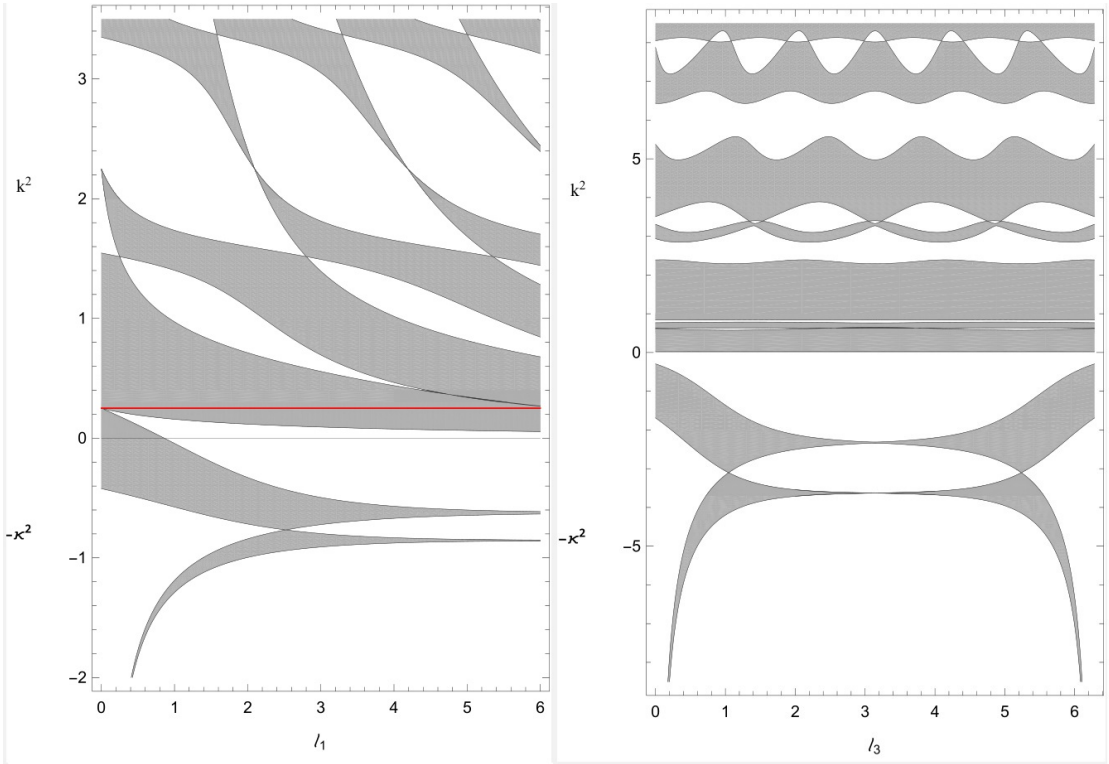

- the probability of belonging to the spectrum, proposed by Band and Berkolaiko [1], for graphs with Kirchhoff vertices

$$P_\sigma(H) := \lim_{K\to\infty} \frac{1}{K} |\sigma(H) \cap [0, K]|$$

[1] R. Band, G. Berkolaiko, Phys. Rev. Lett. 113 (2013).

The magnetic field influences the probability of the limiting cases only:

- loosely connected rings, $\ell_i \neq 0$ ($d_v = 3$): $P_\sigma(H) = 0$.

Baradaran, M., Exner, P. and Tater, M, Ann. Phys. 443 (2022) 168992.

The magnetic field influences the probability of the limiting cases only:

- loosely connected rings, $\ell_i \neq 0$ ($d_v = 3$): $P_\sigma(H) = 0$.
- tightly connected rings, $\ell_1 = 0$ ($d_v = 4$):

$$P_\sigma(H) = \begin{cases} \frac{1}{2} + 2A - 4A^2 \quad (A \bmod \frac{1}{2}) & \ldots \quad \ell_3 \neq \pi\,, \quad \frac{\ell_2}{\ell_3} \notin \mathbb{Q} \\ 1 - \frac{1}{\pi} \arccos(\cos 2A\pi) & \ldots \quad \ell_3 = \pi \end{cases}$$

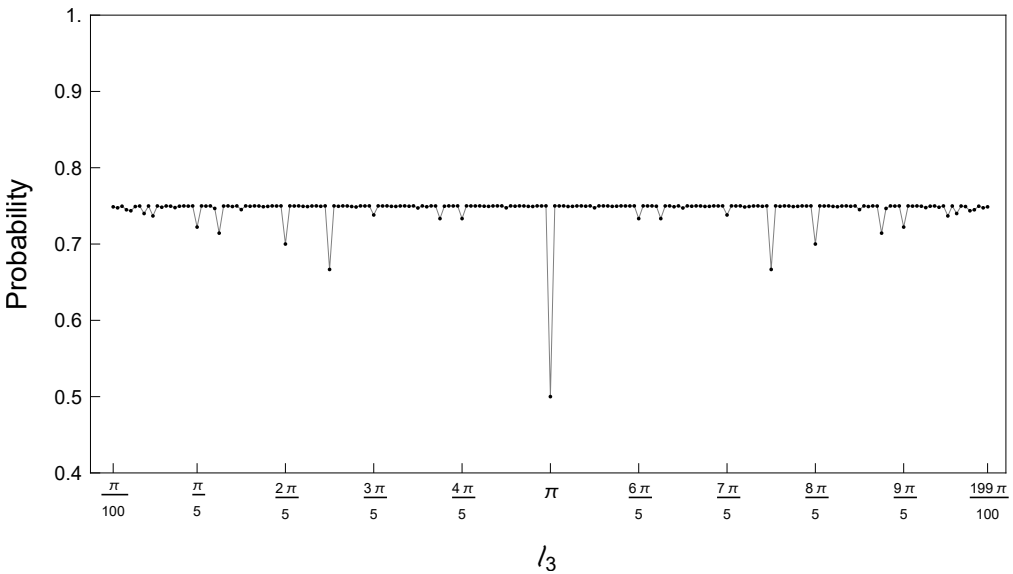

Baradaran, M., Exner, P. and Tater, M, Ann. Phys. 443 (2022) 168992.

The magnetic field influences the probability of the limiting cases only:

- loosely connected rings, $\ell_i \neq 0$ ($d_v = 3$): $P_\sigma(H) = 0$.
- tightly connected rings, $\ell_1 = 0$ ($d_v = 4$):

$$P_\sigma(H) = \begin{cases} \frac{1}{2} + 2A - 4A^2 \quad (A \bmod \frac{1}{2}) & \ldots \quad \ell_3 \neq \pi\,, \ \frac{\ell_2}{\ell_3} \notin \mathbb{Q} \\ 1 - \frac{1}{\pi} \arccos(\cos 2A\pi) & \ldots \quad \ell_3 = \pi \end{cases}$$

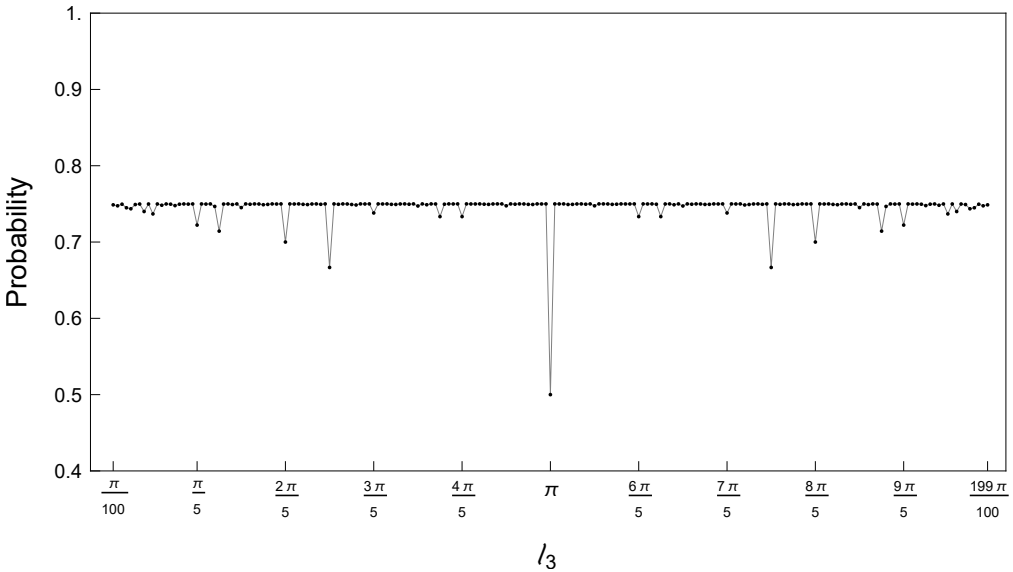

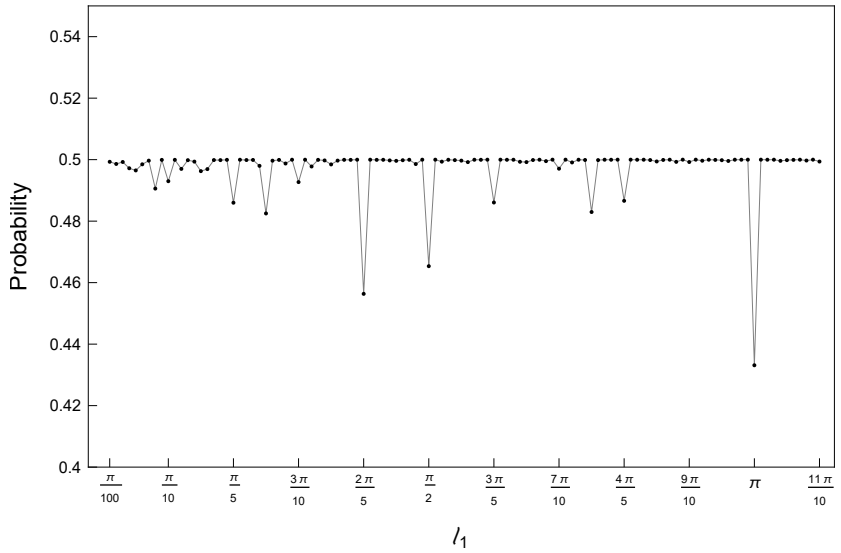

- the limiting case when $\ell_3 = 0$ ($d_v = 4$) and $\ell_1 \notin 2\pi\mathbb{Q}$: $P_\sigma(H) = \frac{1}{2}$.

Baradaran, M., Exner, P. and Tater, M, Ann. Phys. 443 (2022) 168992.

The magnetic field influences the probability of the limiting cases only:

- loosely connected rings, $\ell_i \neq 0$ ($d_v = 3$): $P_\sigma(H) = 0$.
- tightly connected rings, $\ell_1 = 0$ ($d_v = 4$):

$$P_\sigma(H) = \begin{cases} \frac{1}{2} + 2A - 4A^2 \quad (A \bmod \frac{1}{2}) & \ldots \quad \ell_3 \neq \pi\,, \ \frac{\ell_2}{\ell_3} \notin \mathbb{Q} \\ 1 - \frac{1}{\pi} \arccos(\cos 2A\pi) & \ldots \quad \ell_3 = \pi \end{cases}$$

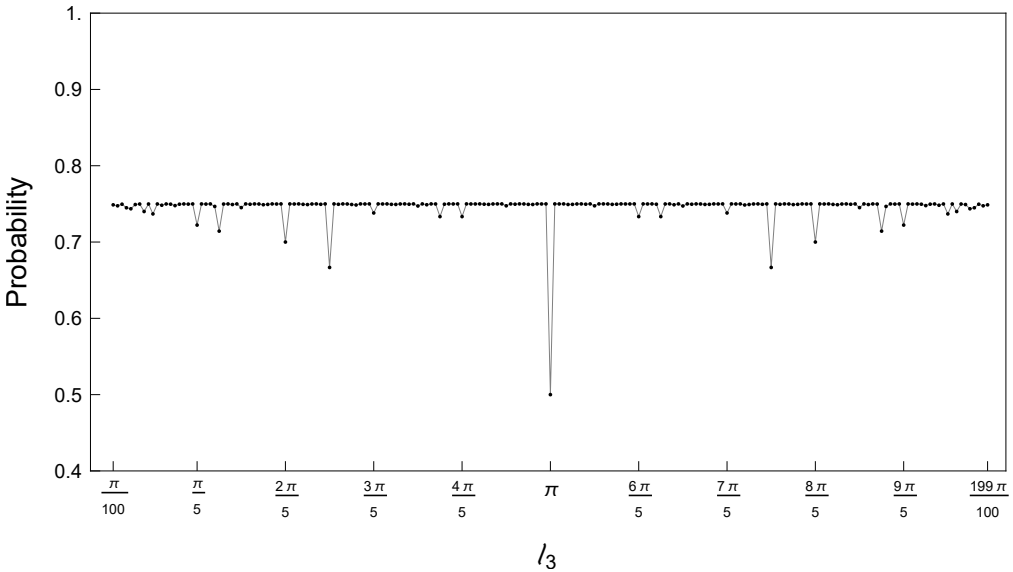

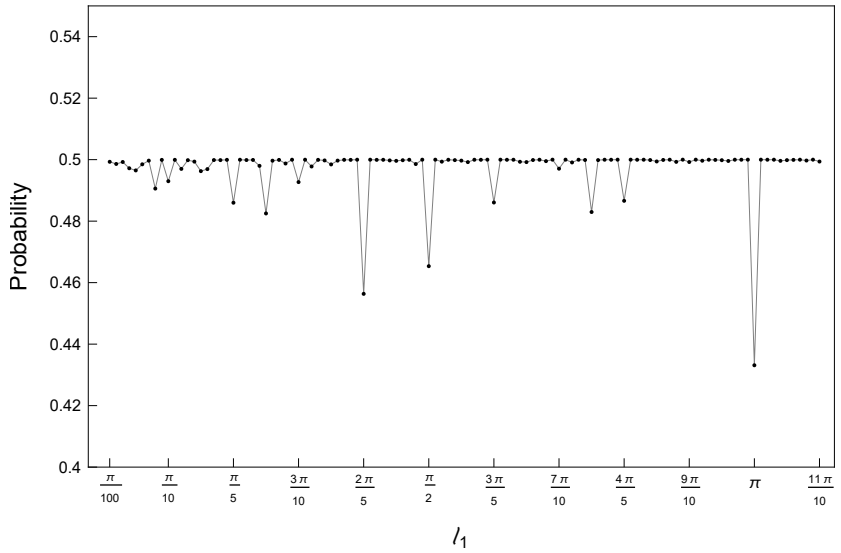

- the limiting case when $\ell_3 = 0$ ($d_v = 4$) and $\ell_1 \notin 2\pi\mathbb{Q}$: $P_\sigma(H) = \frac{1}{2}$.

The Band–Berkolaiko universality holds whenever the edges are incommensurate.

Baradaran, M., Exner, P. and Tater, M, Ann. Phys. 443 (2022) 168992.

Square lattice in a magnetic field $\mathbf{B} = (0, 0, B)$

- the flux per plaquette $\Phi = \frac{p}{q}\,\Phi_0$ with coprime $q \geq 2$ and $p = 1, 2, ..., q-1$; the magnetic unit cell consists of q plaquettes
- we use the Landau gauge $\mathbf{A} = B(0, x, 0)$ for the magnetic potential
- on the horizontal edges,the operator acts as $-\frac{d^2}{dx^2}$; the solutions are combinations of $e^{\pm ikx}$
- on the vertical edges, we have $-\mathcal{D}_v^2 := -\left(\frac{d}{dy} - ivB\right)^2$ where $v = 1, 2, ..., q$ is the vertex index; the solutions are linear combinations of $e^{ivBy}\, e^{\pm iky}$

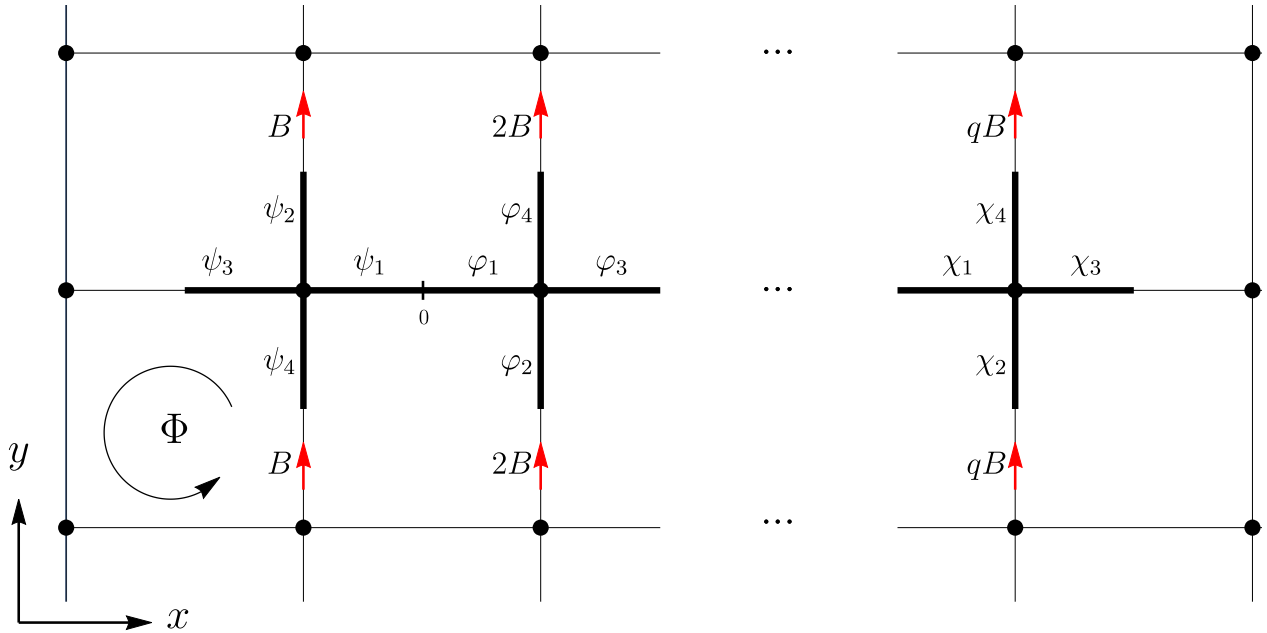

Baradaran, M., Exner, P. and Lipovsky, J., Ann. Phys. 454 (2023) 169339.

The spectral condition is determined by solving a system of $4q$ linear equations.

- band spectrum for $\Phi = \pi$ ($q = 2$ and $p = 1$)

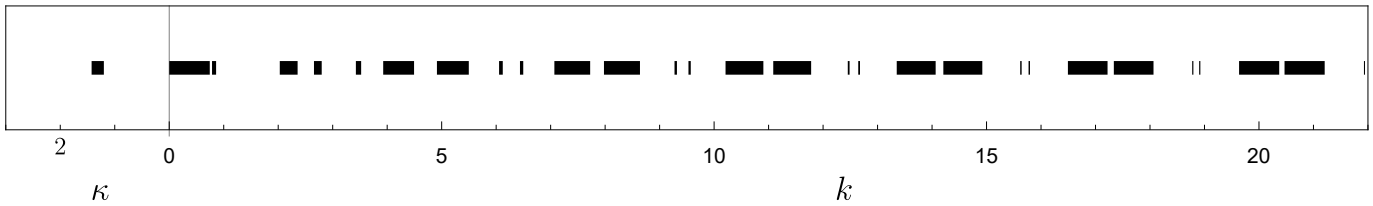

  - pairs of wide bands determined by the condition $-1 \leq \cos 2k \leq 0$
  - pairs of narrow bands in the vicinity of the roots of $\sin^2 k$ of the width $\triangle E_{n,b} = 2(\sqrt{2} - 1) + \mathcal{O}(n^{-2})$ and $\triangle E_{n,g} = 4 + \mathcal{O}(n^{-2})$

The spectral condition is determined by solving a system of $4q$ linear equations.

- band spectrum for $\Phi = \pi$ ($q = 2$ and $p = 1$)

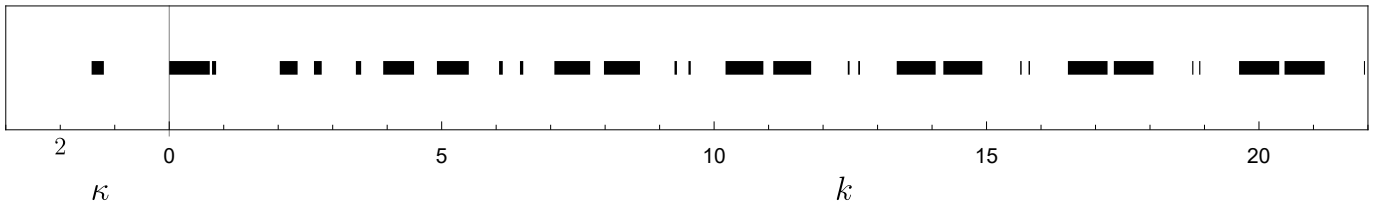

  - pairs of wide bands determined by the condition $-1 \leq \cos 2k \leq 0$
  - pairs of narrow bands in the vicinity of the roots of $\sin^2 k$ of the width $\triangle E_{n,b} = 2(\sqrt{2} - 1) + \mathcal{O}(n^{-2})$ and $\triangle E_{n,g} = 4 + \mathcal{O}(n^{-2})$

- band spectrum for $\Phi = 2\pi\frac{p}{3}$ ($q = 3$ and $p = 1, 2$).

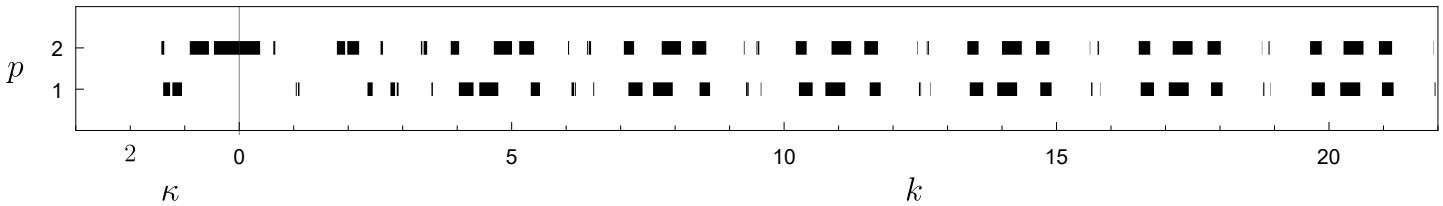

  - series of 'three' wide bands determined by the condition

$$-1 \leq \; -3\cos\left(k + \tfrac{2\pi p}{3}\right) - 3\cos\left(k - \tfrac{2\pi p}{3}\right) - 9\cos k - 4\cos 3k \; \leq 1$$

  - series of 'three' narrow bands with asymptotically constant width

- band spectrum vs. the flux ratio $\frac{\Phi}{\Phi_0} = \frac{p}{q}$ with $q \in \{2, ..., 12\}$ and $p = 1, ..., q-1$

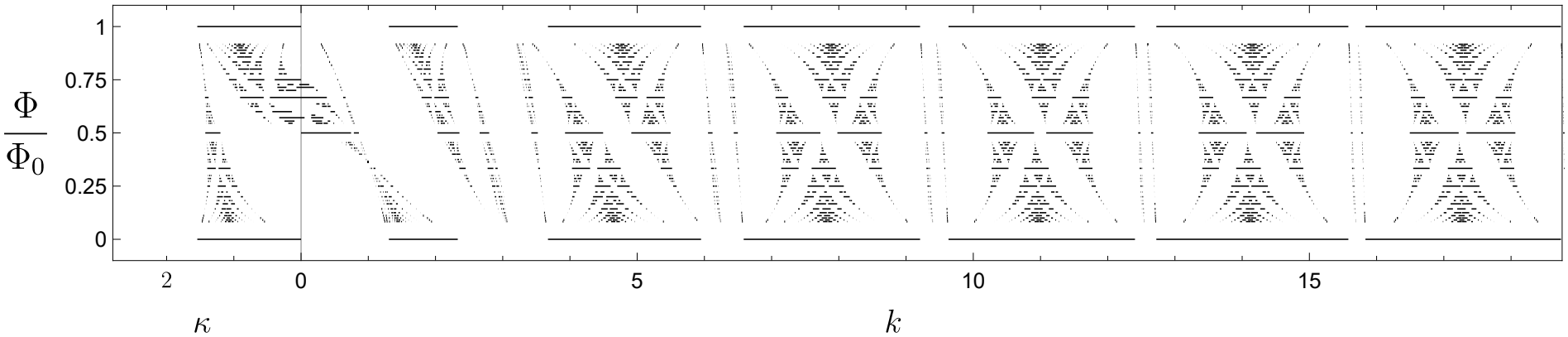

- At low energies, the effect of the vertex condition is dominant.
- in the high-energy regime, it is the magnetic field which dominates restoring asymptotically the familiar Hofstadter's butterfly pattern (or the solution of the almost Mathieu equation)
- there are series of narrow bands, appearing between each pair of butterflies, with asymptotically constant width

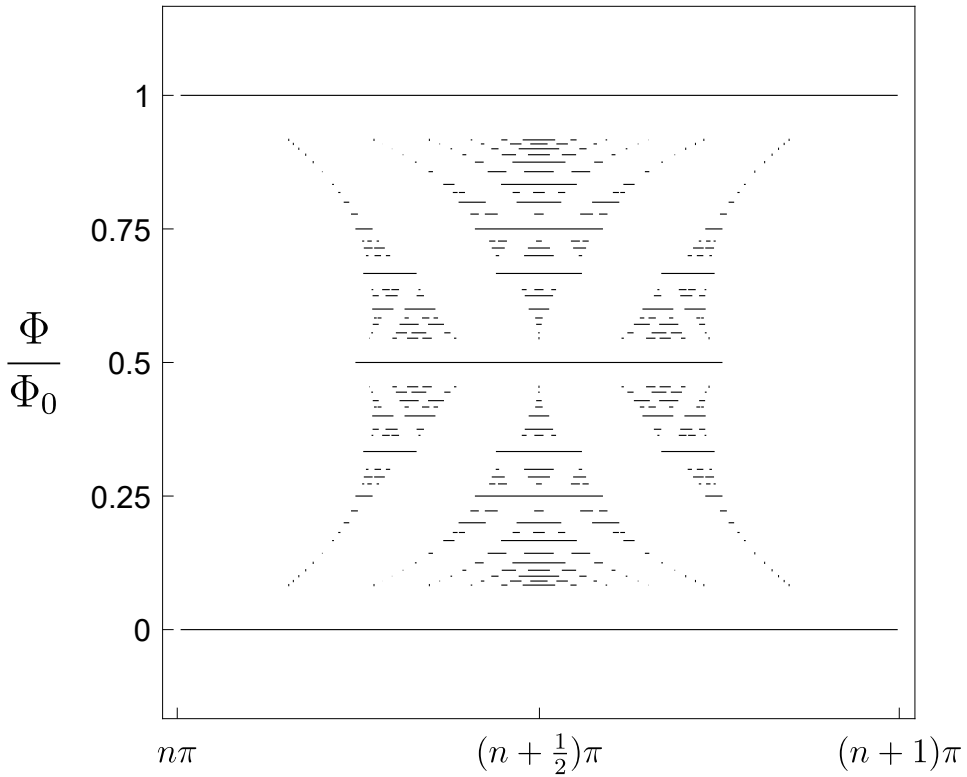

Figure: The asymptotic shape of the butterfly part of the spectrum. At the top and bottom, the spectral bands of the non-magnetic case are shown.

- the probability of belonging to the spectrum, $P_\sigma(H) := \lim_{K\to\infty} \frac{1}{K} |\sigma(H) \cap [0, K]|$

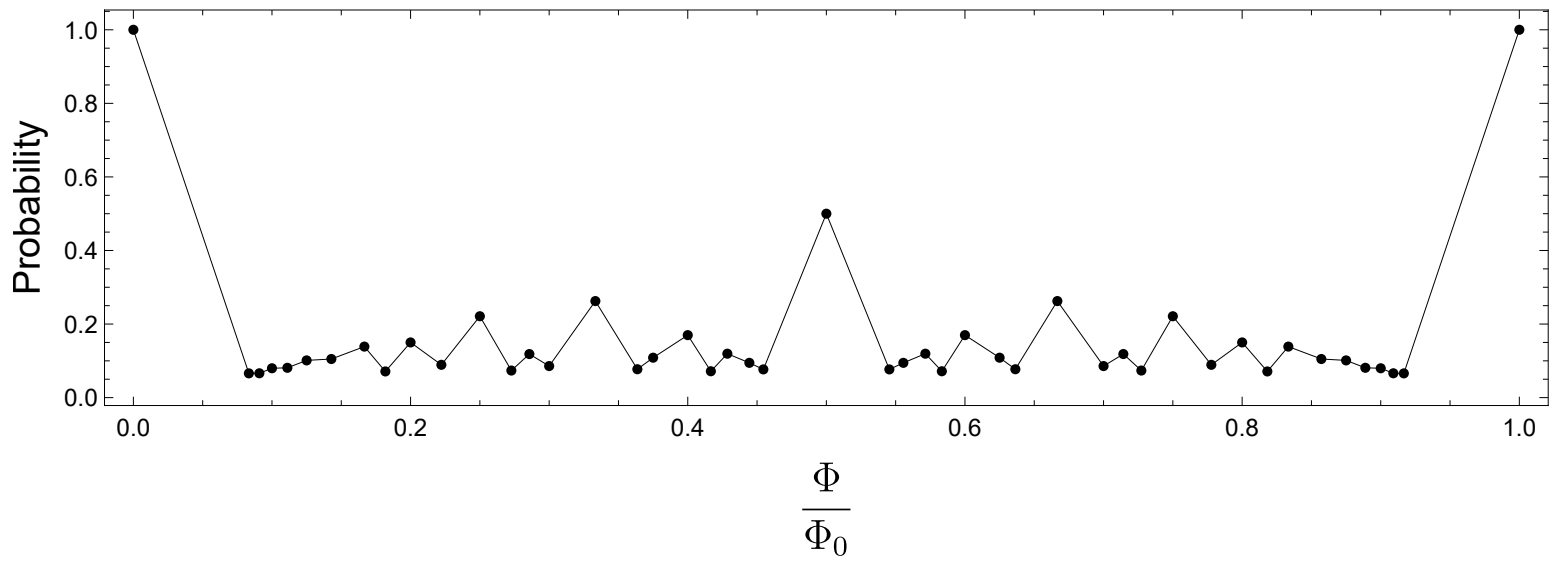

Figure: The probability $P_\sigma(H)$ versus the flux ratio $\frac{\Phi}{\Phi_0} = \frac{p}{q}$ with $q \in \{2, ..., 12\}$ and $p = 1, ..., q-1$.

- with increasing q, the number of bands increases while the probability quantity decreases: the spectrum could be fractal, in fact a Cantor set, for irrational flux ratios

- we compare the obtained probabilities with the Thouless conjecture for the almost Mathieu operator

$$\lim_{q\to\infty} q|\sigma\left(\Phi = 2\pi\frac{p}{q}\right)| = \frac{16\, C_{\mathrm{Cat}}}{\pi}$$

where $C_{\mathrm{Cat}} = \sum_{n\in\mathbb{N}}(-1)^n(2n+1)^{-2} \approx 0.9159...$

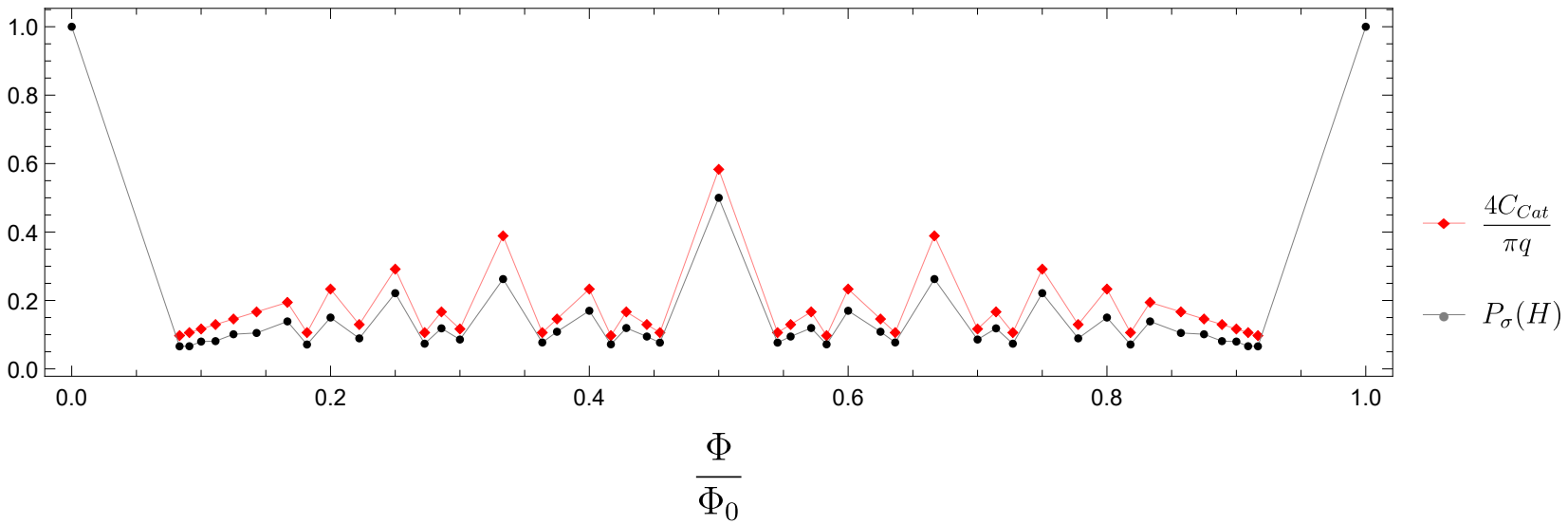

Figure: Comparison of $P_\sigma(H)$ to the Thouless conjecture values indicated by the red diamonds.

A recent modification of the model: Cairo lattice example

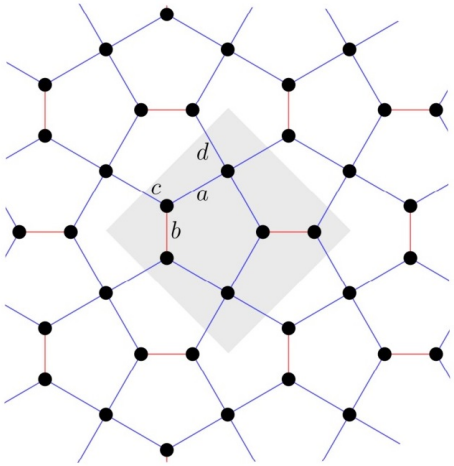

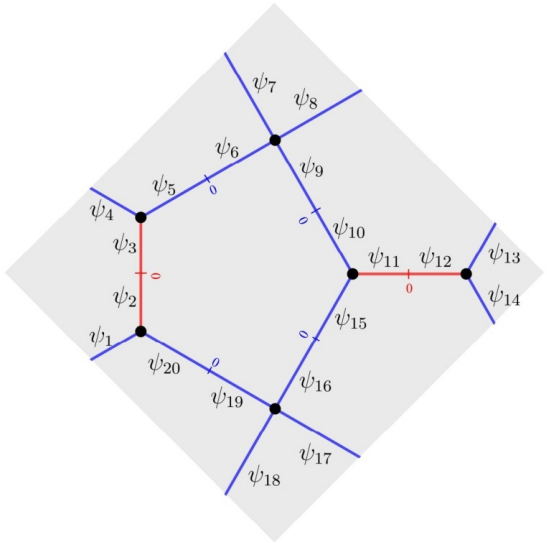

Baradaran, M., Exner, P.,
J. Phys. A: Math. Theor.
57 (2024) 265202.

- we consider a Cairo lattice with the edges lengths a and $b = (\sqrt{3} - 1)a$
- choosing $U = \pm R$, the coupling conditions are

$$\pm(\psi_{j+1} \mp \psi_j) + i\ell_{d_v}\,(\pm\psi'_{j+1} + \psi'_j) = 0, \qquad d_v = 3, 4$$

A recent modification of the model: Cairo lattice example

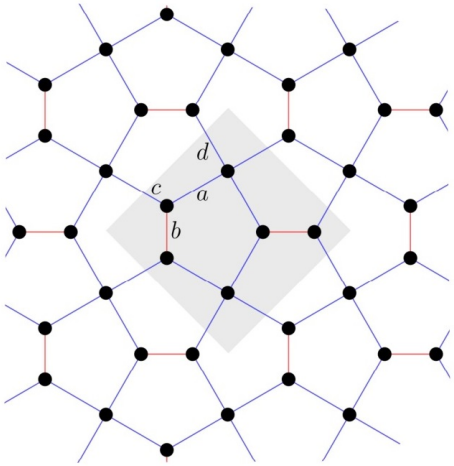

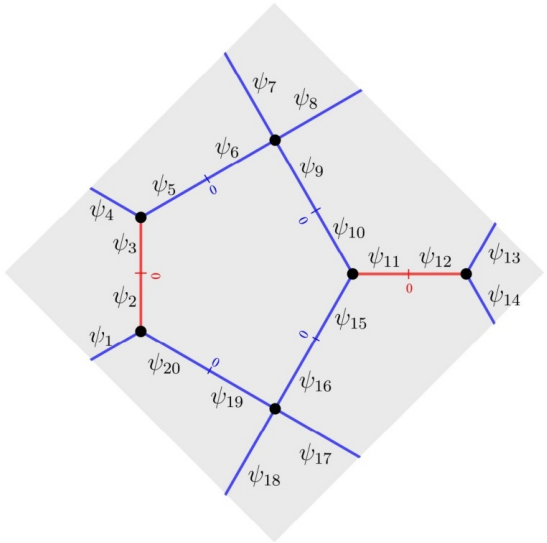

Baradaran, M., Exner, P.,
J. Phys. A: Math. Theor.
57 (2024) 265202.

- we consider a Cairo lattice with the edges lengths a and $b = (\sqrt{3} - 1)a$
- choosing $U = \pm R$, the coupling conditions are

$$\pm(\psi_{j+1} \mp \psi_j) + i\ell_{d_v}\,(\pm\psi'_{j+1} + \psi'_j) = 0, \qquad d_v = 3, 4$$

R coupling at all vertices results in $P_\sigma(H^{+R}_{\ell_3,\ell_4}) = 0$ for any $\ell_3, \ell_4 > 0$

A recent modification of the model: Cairo lattice example

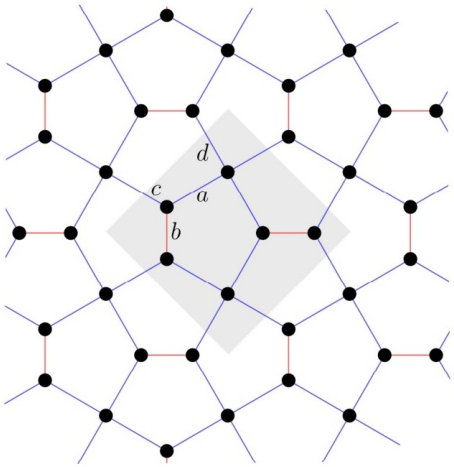

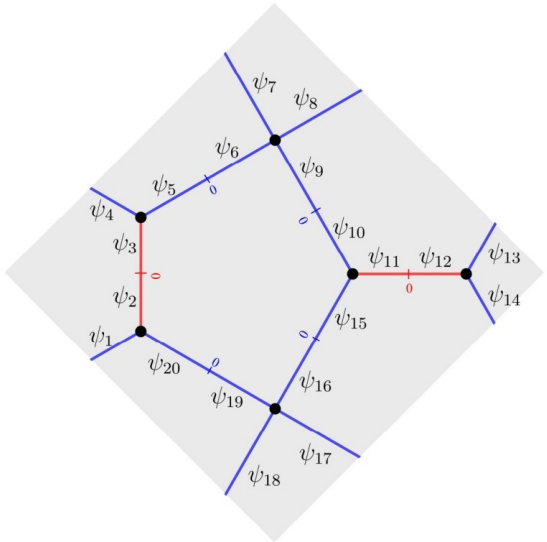

Baradaran, M., Exner, P.,
J. Phys. A: Math. Theor.
57 (2024) 265202.

- we consider a Cairo lattice with the edges lengths a and $b = (\sqrt{3} - 1)a$
- choosing $U = \pm R$, the coupling conditions are

$$\pm(\psi_{j+1} \mp \psi_j) + i\ell_{d_v}\,(\pm\psi'_{j+1} + \psi'_j) = 0, \qquad d_v = 3, 4$$

R coupling at all vertices results in $P_\sigma(H^{+R}_{\ell_3,\ell_4}) = 0$ for any $\ell_3, \ell_4 > 0$

1. the limit $\ell_3 \to 0$, changes the R coupling to the Kirchhoff one; $P_\sigma(H^{+R}_{0,\ell_4}) \approx 0.82$
2. imposing R at $d_v = 4$ and $-R$ at $d_v = 3$, again, we get $P_\sigma(H^{\pm R}_{\ell_3,\ell_4}) \approx 0.82$

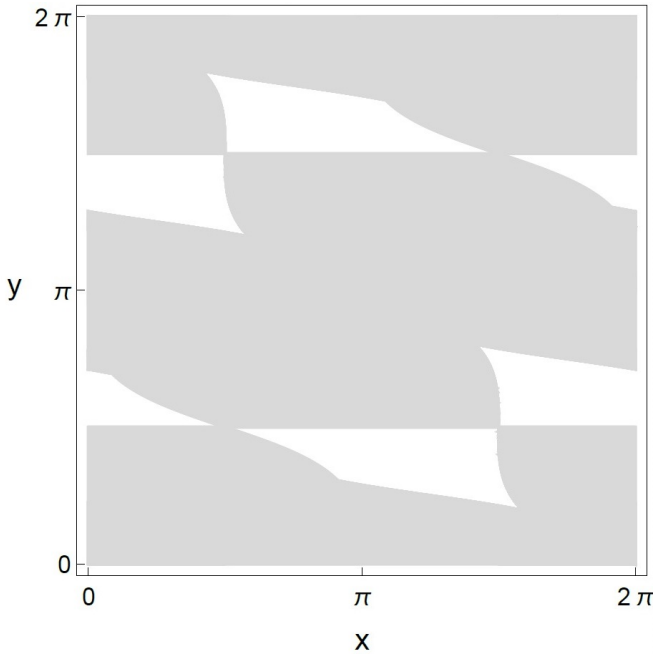

(a) the model with R coupling in the limit $\ell_3 \to 0$

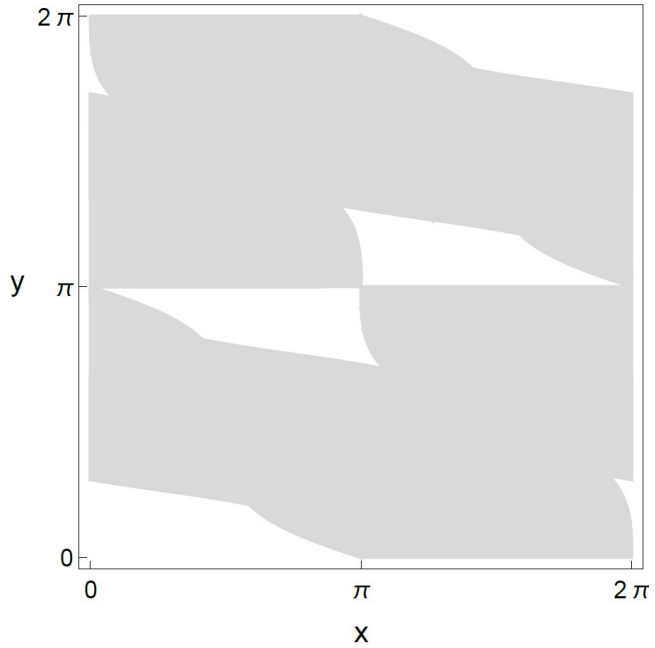

(b) the model with $(-1)^{d_v} R$ coupling

Figure 1: The grey shaded area equals to $4\pi^2 P_\sigma(H)$; the axes correspond to $x := \sqrt{3}\, ka$ and $y := ka$ in the high-energy regime $k \to \infty$.

This conclusion is not only numerical; we see that the asymptotic conditions giving rise to these regions are obtained one from the other through the transformations $x \leftrightarrow x + \frac{\pi}{2}$ and $y \leftrightarrow y - \frac{\pi}{2}$.

Baradaran, M., Exner, P., J. Phys. A: Math. Theor. 57 (2024) 265202.

Thank you for your attention!